



Research paper

Stationary states of systems with intermolecular interactions dominated by electrostatics: Structure of trimethylammonium and tetramethylammonium chlorides and bromides in the gas phase, monomers and dimers

Gleb S. Denisov^a, Hans-Heinrich Limbach^b, Ibon Alkorta^{c,*}, José Elguero^c

^a Department of Physics, St. Petersburg State University, St. Petersburg 198504, Russia

^b Institut für Chemie und Biochemie, Freie Universität Berlin, 14195 Berlin, Germany

^c Instituto de Química Médica (CSIC), Juan de la Cierva, 3, E-28006 Madrid, Spain



ARTICLE INFO

Keywords:

Non-covalent interactions

Hydrogen bonds

Tetrel bonds

Vibrational spectra

ABSTRACT

This work reports the theoretical study carried out with the M06-2x functional and the aug-cc-pVTZ basis set of four ammonium and two phosphonium salts, $\text{Me}_3\text{NH}^+\text{Cl}^-$, $\text{Me}_3\text{NH}^+\text{Br}^-$, $\text{Me}_4\text{N}^+\text{Cl}^-$, $\text{Me}_4\text{N}^+\text{Br}^-$, $\text{Me}_4\text{P}^+\text{Cl}^-$ and $\text{Me}_4\text{P}^+\text{Br}^-$. The structure of the monomeric and dimeric complexes (between 1 and 5 conformations each) has been analyzed in what concern geometries, energies and NH^+ stretching frequencies. The ammonium geometries were successfully compared with the X-ray structures found in the CSD.

1. Introduction

The structure of tertiary and quaternary ammonium salts has been the object of many studies starting from old times since these compounds are archetypical organic equivalent to inorganic salts of the sodium chloride class [1,2]. The main structural difference between these classes is that only tertiary salts are able to form hydrogen bonds (HBs) [3]. Quaternary salts are much more important than tertiary ones in biology (acetylcholine) and in applications (detergents, surfactants, antimicrobial, disinfectants).

Tertiary salts of general formula $\text{R}_3\text{NH}^+\text{X}^-$ (R groups can be identical or different) have been the subjects of many structural and spectroscopic studies. They include conductance studies of R_3NH -picrates and the effect of the addition of amines mediated by HBs [4,5]. Electrical dipole-dipole interactions and ion pairs were studied by IR and dynamic ^1H NMR (DNMR) [6–8]. A combination of IR and ^1H NMR was used in the case of tributylammonium salts [9]. NH and ND distances of trimethylammonium chloride were obtained by dipolar ^{15}N solid state NMR [10]. The use of IR predissociation (IRPD) spectroscopy allows one to record the IR spectra using a mass spectrometer of the isolated Me_3NH^+ cation without the counterion but with several neutral proton acceptors. For instance, the $\text{Me}_3\text{NH}^+\cdots\text{X}$ dimer with $\text{X} = \text{argon}$ shows a $\nu_{\text{N-H}^+}$ peak at 3278 cm^{-1} [11].

Due to its importance, the bibliography concerning quaternary salts

is very large: their interaction with nitriles has been studied [12,13]; X-ray crystallography including polymorphism [14] and solvates with nitriles [13]; their use as chiral catalysts [15] and within receptors (acetylcholine) [16]. Amongst the theoretical studies, the complexes of quaternary ammonium cations (tetramethyl, trimethylethyl, choline and acetylcholine) with OH^- , F^- and Cl^- were studied at the B3LYP and MP2 levels: stable structures correspond to ones where the anion is bonded to the three H atoms directed away from the cationic head on each of three methyl groups [17]. A more recent paper reported the structural and dynamic properties of tetraalkyl-ammonium bromide aqueous solutions [18]. Finally, there is one paper in 2020 on the fluorination of 2-bromobenzonitrile by means of tetramethylammonium fluoride ($\text{Me}_4\text{N}^+\text{F}^-$) [19]. In this paper $\text{Me}_4\text{N}^+\text{F}^-$ was calculated at the 6-31+G(d) using the X3LYP functional of Goddard [20]; monomer, dimer and tetramer of $\text{Me}_4\text{N}^+\text{F}^-$ were calculated.

2. Computational methods

The geometry of the systems has been optimized with the M06-2x functional and the aug-cc-pVTZ basis set. Frequency calculations have been carried out to confirm that the systems obtained correspond to energetic minima. For the infrared spectra, the harmonic frequencies have been scaled by a factor of 0.9679 [21]. These calculations have been carried out with the Gaussian-16 program [22]

* Corresponding author.

E-mail address: ibon@iqm.csic.es (I. Alkorta).

<https://doi.org/10.1016/j.cplett.2021.138809>

Received 16 May 2021; Received in revised form 2 June 2021; Accepted 3 June 2021

Available online 6 June 2021

0009-2614/© 2021 The Author(s).

Published by Elsevier B.V. This is an open access article under the CC BY-NC-ND license

(<http://creativecommons.org/licenses/by-nc-nd/4.0/>).

The electron density of the systems has been analyzed within the Quantum Theory of Atoms in Molecules (QTAIM) methodology [23,24] and the interactive quantum atoms (IQA) partition method [25] has been used to analyze the interatomic energies with the AIMAll program [26].

3. Results and discussion

We will consider only the cases of chlorides and bromides, by far the most studied. The iodides need relativistic corrections [27,28] and the fluorides, like $\text{Me}_4\text{P}^+\text{F}^-$, exists in a pentavalent form, according to Kornath [29]. All the optimized geometries are reported in the Supplementary Material (Table S1).

3.1. The trimethylammonium cation, Me_3NH^+ , and its salts $\text{Me}_3\text{NH}^+\text{X}^-$

3.1.1. Energetic aspects

The isolated Me_3NH^+ cation **1a** presents C_{3v} symmetry with a calculated NH distance of 1.021 Å (Fig. 1a). Three minima have been found in the $\text{Me}_3\text{NH}^+\text{X}^-$ potential energy surface (Fig. 1b, 1c and 1d). The most stable one **1b** corresponds to the interaction of X^- with the NH group and can be envisioned as the complex formed by the Me_3N and HX. In fact, at the computational method used here, the hydrogen bond complex **1b** spontaneously evolves towards the proton transfer complex in agreement with the experimental microwave spectroscopy results [30]. The binding energies of complexes **1b** are very large (−490 and −462 $\text{kJ}\cdot\text{mol}^{-1}$ as expected for the interaction between an anion and a cation.

The second minimum found for the $\text{Me}_3\text{NH}^+\text{X}^-$ complexes corresponds to the interaction of the anion with the three methyl groups simultaneously (**1c**). These minima are 73 and 67 $\text{kJ}\cdot\text{mol}^{-1}$ less stable than (**1b**) for $\text{X} = \text{Cl}$ and Br, respectively. The comparison of **1c** with the isolated Me_3N plus HX showed that for $\text{X} = \text{Cl}$ (**1c**) is less stable by 6 $\text{kJ}\cdot\text{mol}^{-1}$ while for $\text{X} = \text{Br}$ it is more stable by 18 $\text{kJ}\cdot\text{mol}^{-1}$.

The last minimum (**1d**) shows an interaction of the anion with a single methyl group. It is the least stable minimum with relative energies to the most stable minimum of 151 and 137 $\text{kJ}\cdot\text{mol}^{-1}$ for $\text{X} = \text{Cl}$ and Br, respectively.

Using the minima located for the $\text{Me}_3\text{NH}^+\text{X}^-$ system, four minima have been build and optimized for $(\text{Me}_3\text{NH}^+\text{X}^-)_2$ (Fig. 2).

The energetics of these systems indicates that complexes **2a-2c** are stabilized with respect to the dissociation in two **1b** complexes (Table 1 while conformer **2d** is the less stable. For the same conformation, the stabilization of the bromide derivatives is slightly larger than the

chloride ones (between 2 and 4 $\text{kJ}\cdot\text{mol}^{-1}$).

3.1.2. Geometrical and electron density aspects

A variety of intermolecular interactions are present in the systems studied. They include standard $\text{NH}\cdots\text{X}$ hydrogen bonds, $\text{CH}\cdots\text{X}$, $\text{H}\cdots\text{H}$, $\text{C}\cdots\text{X}$, and $\text{X}\cdots\text{X}$ contacts which present the corresponding bond critical point (BCP) in the AIM analysis. The molecular graphs derived from the electron density analysis of the isolated **1a** and the **1b** minima are shown in Fig. 1 and those of the $(\text{Me}_3\text{NH}^+\text{Cl}^-)_2$ dimers are gathered in Fig. 2. The analogous molecular graphs of $\text{Me}_3\text{NH}^+\text{Br}^-$ are gathered in the SM (Fig. S1). The IQA methodology has been used to identify the attractive or repulsive nature of such interactions.

3.1.2.1. Classical hydrogen bonds $\text{N}^+\text{H}\cdots\text{X}^-$. The N^+H distance in isolated Me_3NH^+ (**1a**) is 1.021 Å. In the monomeric complexes, $\text{Me}_3\text{NH}^+\text{Cl}^-$ and $\text{Me}_3\text{NH}^+\text{Br}^-$ they are 1.166 and 1.120 Å, respectively. Thus the elongation is greater for the chloride than the bromide, as expected [31,32]. For polycrystalline trimethylammonium chloride an N^+H distance of 1.093 Å has been observed for $(\text{CD}_3)_3\text{NH}^+\text{Cl}^-$ as well as an ND^+ distance of 1.079 Å for $(\text{CH}_3)_3\text{ND}^+\text{Cl}^-$ by dipolar ^{15}N solid state NMR [10]. The calculated value is 0.073 Å longer than the experimental value probably due to phase effects. Thus, the N^+H distance in the two more stable dimers **2a** and **2b**, with $\text{X} = \text{Cl}$, is reduced to 1.074 and 1.105 Å, respectively, as clear indication that the presence of more molecules tend to reduce this distance. Similar results are obtained for $\text{X} = \text{Br}$, where the N^+H distance in **2a** and **2b** are 1.058 and 1.086 Å, respectively.

3.1.2.2. $\text{C}\cdots\text{X}^-$ Hydrogen bonds of the methyl groups in **1c and **1d**.** The elongation of the $\text{C}\cdots\text{H}$ bonds of the three methyl groups pointed to the anion can be estimated by comparison with the remaining hydrogens not involved in the HBs. Obviously, the effects are much weaker than those involving the N^+H group, but the effect has the same sign in average, 0.0055 Å for Cl^- and 0.0045 Å for the Br^- , respectively. The effects are weaker for phosphonium than for ammonium, also as expected, about by 0.0025 Å [33].

3.1.2.3. $\text{X}^-\cdots\text{X}^-$ and $\text{C}\cdots\text{C}$ interactions (halogen and tetrel bonds). In the AIM analysis appear two (BCPs) that are very unusual: monoatomic anion-anion interaction in complexes **2a** with values of 4.176 Å for the chloride and 4.295 Å for the bromide. The IQA analysis of **2a** shows attractive terms between associated to the $\text{X}^-\cdots\text{H}\cdots\text{N}$ BCPs (−192.0 and −157.9 $\text{kJ}\cdot\text{mol}^{-1}$ for $\text{X} = \text{Cl}$ and Br, respectively) and $\text{X}^-\cdots\text{HC}$ ones (−41.6 and −37.5 $\text{kJ}\cdot\text{mol}^{-1}$ each contact) while repulsive interatomic energies

	1a, Me_3NH^+	1b, $\text{Me}_3\text{NH}^+\text{Cl}^-$	1c, $\text{Me}_3\text{NH}^+\text{Cl}^-$	1d, $\text{Me}_3\text{NH}^+\text{Cl}^-$
μ	0.8	$\text{X} = \text{Cl}$, 8.2 $\text{X} = \text{Br}$, 9.3	$\text{X} = \text{Cl}$, 11.7 $\text{X} = \text{Br}$, 12.6	$\text{X} = \text{Cl}$, 17.2 $\text{X} = \text{Br}$, 17.9
ν_{NH}	3459	$\text{X} = \text{Cl}$, 1585 $\text{X} = \text{Br}$, 1995	$\text{X} = \text{Cl}$, 3493 $\text{X} = \text{Br}$, 3489	$\text{X} = \text{Cl}$, 3478 $\text{X} = \text{Br}$, 3477

Fig. 1. Molecular graphs of the structures of: a) Me_3NH^+ (**1a**), b) $\text{Me}_3\text{NH}^+\text{X}^-$ (**1b**), c) $\text{Me}_3\text{NH}^+\text{X}^-$ (**1c**) and d) $\text{Me}_3\text{NH}^+\text{X}^-$ (**1d**). The figures correspond to $\text{X} = \text{Cl}$ (Fig. S1 gathers the molecular graphs for $\text{X} = \text{Br}$). The location of the bond, ring and cage critical points is indicated with green, red, and blue dots, respectively. μ Dipole moments (Debye) and ν_{NH} stretching frequencies (cm^{-1}) are also given.

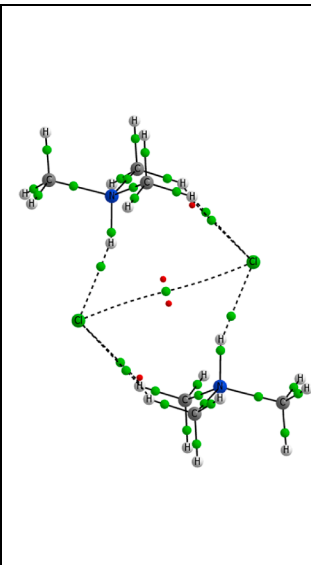
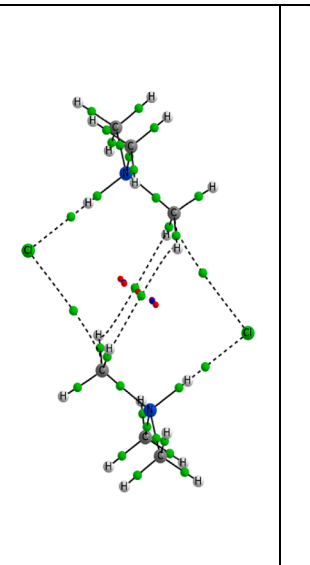
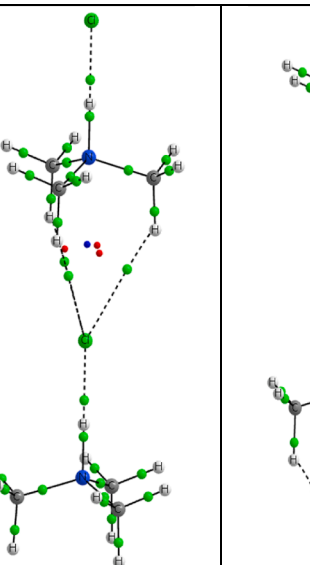
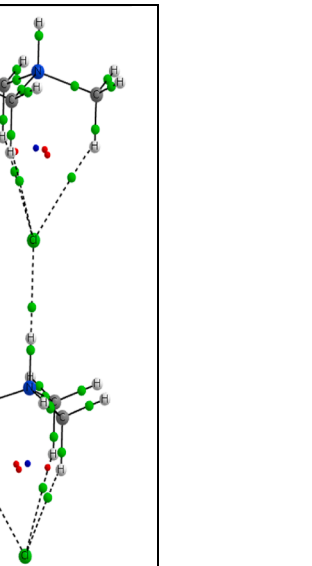
				
	2a , (Me ₃ NH ⁺ Cl ⁻) ₂	2b , (Me ₃ NH ⁺ Cl ⁻) ₂	2c , (Me ₃ NH ⁺ Cl ⁻) ₂	2d , (Me ₃ NH ⁺ Cl ⁻) ₂
μ	0.0	0.0	X = Cl, 20.2 X = Br, 22.0	X = Cl, 28.0 X = Br, 29.8
ν_{NH}	X = Cl, 2594 (asym.), 2567 (sym.) X = Br, 2825 (asym.), 2812 (sym.)	Cl, 2171 (asym.), 2116 (sym.) Br, 2430 (asym.), 2391 (sym.)	Cl, 2075 (asym.), 2010 (sym.) Br, 2328 (asym.), 2286 (sym.)	Cl, 3483 (asym.), 3099 (sym.) Br, 3482 (asym.), 3139 (sym.)

Fig. 2. Molecular graphs of the structures corresponding to the (Me₃NH⁺X⁻)₂ minima. The figures correspond to X = Cl. ν_{NH} Stretching frequencies (cm⁻¹) are also given.

Table 1

Binding energy (kJ·mol⁻¹) of the (Me₃NH⁺X⁻)₂ versus two times Me₃NH⁺X⁻ (1b).

X	(Me ₃ NH ⁺ X ⁻) ₂ (2a)	(Me ₃ NH ⁺ X ⁻) ₂ (2b)	(Me ₃ NH ⁺ X ⁻) ₂ (2c)	(Me ₃ NH ⁺ X ⁻) ₂ (2d)
Cl	-84.9	-52.7	-39.5	+55.7
Br	-87.9	-57.0	-41.6	+45.3

between the two halogen atoms are found with values of +109.7 and +102.8 kJ·mol⁻¹ for X = Cl and Br, respectively. Similar results for monoatomic anion-anion connected by a BCP are described in the literature [34,35] while those in stable polyatomic anion-anion minima have been described as locally attractive [36–38]. In **2b**, attractive interactions associated to the X⁻...H⁻...N⁺ contacts (-217.9 and -185.3

kJ·mol⁻¹) and tetrel X⁻...C bond (-54.5 and -51.8 kJ·mol⁻¹) are found. Each of the H...H contact has only a very minor stabilization contribution (-0.4 kJ·mol⁻¹ for both X = Cl and Br).

3.2. The tetramethylammonium cation, (Me₄N⁺) and its salts (Me₄N⁺X⁻), X = Cl, Br

The tetramethylammonium cation (**3a**) shows *T_d* symmetry with four identical methyl groups surrounding the nitrogen atom (Fig. 3a). Two minima have been found for the Me₄N⁺X⁻ systems. The most stable minimum **3b** is trisector to three methyl groups while the second minimum **3c** is trisector to a single methyl group (Fig. 3b and c). In both cases, the symmetry of **3b** and **3c** is *C_{3v}*. Complex **3b** shows interaction energies of -406 and -386 kJ·mol⁻¹ and they are 74 and 67 more stable than **3c** for X = Cl and Br, respectively. The interatomic N...X distances

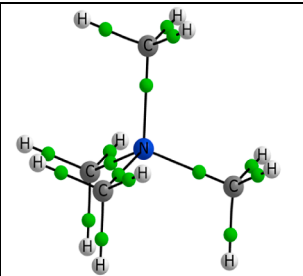
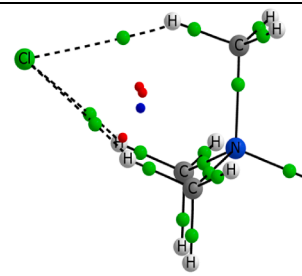
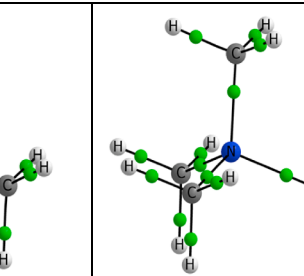
			
	3a , Me ₄ N ⁺	3b , Me ₄ N ⁺ Cl ⁻	3c , Me ₄ N ⁺ Cl ⁻
μ	0.0	X = Cl, 12.4 X = Br, 13.2	X = Cl, 17.3 X = Br, 18.0

Fig. 3. Molecular graphs of the structures of: a) Me₄N⁺ (**3a**), b) Me₄N⁺X⁻ (**3b**) and c) Me₄N⁺X⁻ (**3c**). The figures correspond to X = Cl.

are 3.527 (3.726) and 4.355 (4.527) Å for **3b** and **3c**, respectively, with $X = \text{Cl}$ (Br).

Five minima have been found for the $(\text{Me}_4\text{N}^+\text{X}^-)_2$ dimers (Fig. 4) and their binding energies are reported in Table 2. The order of stability is $a > b > c > d > e$ for both anions; the values being very similar. Dimer **4a** has the same structure as the $\text{Me}_4\text{N}^+\text{F}^-$ dimer [19].

3.2.1. The tetramethylphosphonium cation, (Me_4P^+) and its salts $(\text{Me}_4\text{N}^+\text{X}^-)$, $X = \text{Cl}, \text{Br}$

A single minimum has been found for both the $\text{Me}_4\text{P}^+\text{X}^-$ and $(\text{Me}_4\text{P}^+\text{X}^-)_2$ systems (Fig. 5). These phosphonium structures correspond to the ammonium structures **3a**, **3b** and **4a**. The calculated binding energies of **5b** are -410.3 and -389.2 $\text{kJ}\cdot\text{mol}^{-1}$ for $X = \text{Cl}$ and Br, respectively and the binding energy of **5c** with respect to two times **5b** are -129.0 and -133.4 $\text{kJ}\cdot\text{mol}^{-1}$.

3.3. N–H Stretching frequencies

Figs. 1 and 2 contain the stretching frequencies of the NH groups of $\text{Me}_3\text{NH}^+\text{X}^-$ complexes, monomers and dimers, respectively. The eleven values of chlorides and bromides are related: $\text{Br}^- = 719 + 0.79\cdot\text{Cl}^-$ ($R^2 = 0.997$) as indication of the analogous character of the interactions but modulated by the nucleophilic properties of each anion. For dimers (Fig. 2) having two NH groups, they appear as one symmetric and one antisymmetric vibration.

One of us [6] has reported the behavior of trioctylammonium chloride in CCl_4 at different concentrations. The effect of the concentration was interpreted as the monomer existing in diluted conditions and a dimer existing at higher concentrations. The measured values are for chloride 2050 cm^{-1} (monomer) and 2400 cm^{-1} (dimer) and for the bromide 2300 cm^{-1} (monomer) and 2500 cm^{-1} (dimer). These values correspond to 350 cm^{-1} and 200 cm^{-1} shifts for Cl^- and Br^- , respectively.

Our values (methyl in lieu of octyl and gas phase instead of carbon tetrachloride) are much lower but the two differences are in the same direction. They correspond to “Our calculations” = $0.573 \times$ “Experimental results”.

There has been a recent paper where the ν_{NH} stretching of Me_3NH^+ cation (without a counteranion) has been measured in the gas phase [11]. Using IR predissociation (IRPD) spectroscopy and MP2/aug-cc-

Table 2
Energetics ($\text{kJ}\cdot\text{mol}^{-1}$).

	X = Cl		X = Br	
	Erel ^a	Eb ^b	Erel	Eb ^b
$(\text{Me}_4\text{N}^+\text{X}^-)_2$ (4a)	0.0	-141.4	0.0	-142.6
$(\text{Me}_4\text{N}^+\text{X}^-)_2$ (4b)	25.1	-116.4	26.2	-116.4
$(\text{Me}_4\text{N}^+\text{X}^-)_2$ (4c)	67.5	-73.9	65.1	-77.5
$(\text{Me}_4\text{N}^+\text{X}^-)_2$ (4d)	93.5	-47.9	95.0	-47.6
$(\text{Me}_4\text{N}^+\text{X}^-)_2$ (4e)	155.2	13.8	150.7	8.1

^a Relative energy with respect to the most stable $(\text{Me}_4\text{N}^+\text{X}^-)_2$ dimer.

^b Energetic difference between these complexes and two isolated $\text{Me}_4\text{N}^+\text{X}^-$ (**3b**)

pVDZ calculations the authors established that Me_3NH^+ associated with different molecules shows Fermi splitting bands in the case of CO, C_2H_2 , H_2O , MeOH and EtOH but not in the case of Ar ($\nu_{\text{N-H}^+} = 3278$ cm^{-1}) and N_2 ($\nu_{\text{N-H}^+} = 3265$ cm^{-1}). The authors indicate that their values are related to the seven molecules proton affinities. We carried a linear regression with their data and found an intercept (PA = 0) of 3513 cm^{-1} . This value that corresponds to the absence of association agrees with our value (3459 cm^{-1} , Fig. 1).

3.4. Comparison with X-ray structures

To answer the question if the structures calculated for the gas phase bear some similitude with those determined by X-ray crystallography, a search in the CSD [39] was carried out. The emphasis was put on arrangement more than in distances and angles. In the years 2018–2020 the X-ray structures of $\text{Me}_3\text{NH}^+\text{Cl}^-$, $\text{Me}_3\text{NH}^+\text{Br}^-$, $\text{Me}_4\text{N}^+\text{Cl}^-$ and $\text{Me}_4\text{N}^+\text{Br}^-$ were published (see Table S2). It is possible to find fragments of these crystal structures, cutting them in different ways, that resemble the complexes we have reported in the previous sections of this article. For instance in the crystal structures of $\text{Me}_3\text{NH}^+\text{Cl}^-$ (TMAMMC03 [40]) and $\text{Me}_3\text{NH}^+\text{Br}^-$ (ZZZGVM03 [41]) fragments similar to complexes **1b**, **1c** and **1d** of Fig. 1 were found. The same happens for $(\text{Me}_3\text{NH}^+\text{X}^-)_2$ (Fig. 2) where fragments corresponding to **2a**, **2b**, **2c** and **2d** were found both for Cl^- and for Br^- .

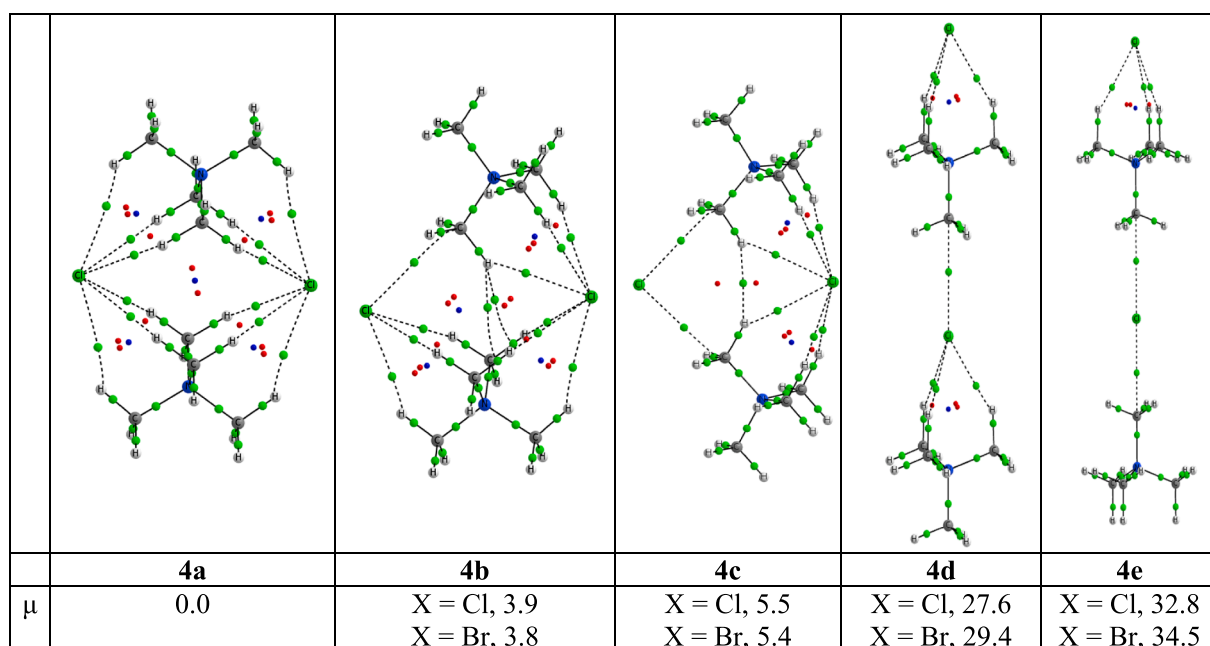


Fig. 4. Molecular graphs of the structures of $(\text{Me}_4\text{N}^+\text{X}^-)_2$ minima. The figures correspond to $X = \text{Cl}$.

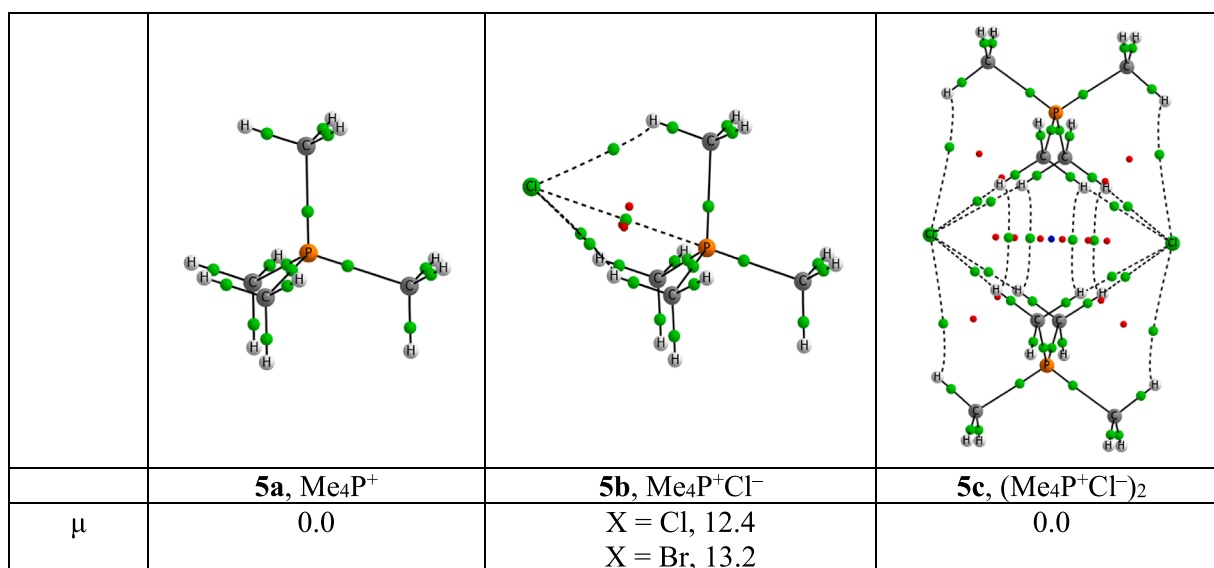


Fig. 5. Molecular graphs of the structures of Me₄P⁺, Me₄P⁺Cl⁻ and (Me₄P⁺Cl⁻)₂.

In the case of Me₄N⁺Cl⁻ (ZZZUQM02 [42]) and Me₄N⁺Br⁻ (ZZZUQO04 [43]) situations similar to those represented in Fig. 3 and Fig. 4 have been found. For chloride, **4a**, a new dimeric motive is present in the crystal of ZZZUQM02; this dimer in the gas phase calculations has one imaginary frequency. Its existence in the crystal is probably due to intermolecular interactions with surrounding molecules that stabilize it and that are absent in the calculated monomer. Also for the bromide **4a** there is a dimer with one imaginary frequency that is present in the ZZZUQO04 crystal.

In summary, an unexpected good agreement exists between crystal structures and gas phase calculations.

4. Conclusions

We have explored the non-covalent interactions in trimethylammonium and tetramethylammonium chlorides and bromides by theoretical calculations in the gas phase, mainly but not only, hydrogen bonds [44]. The trimethylammonium cation was selected as the simplest ammonium cation with only one HB to avoid multiples HBs. Note that the tetramethylammonium cation is the product of the Menshutkin reaction between MeCl and Me₃N. Both types of cations are representative of the chemistry of ammonium salts, including amino acids in their zwitterionic forms. Comparing the calculations with the available experimental data results in a more than satisfactory agreement.

The quaternary phosphonium salts present a much-simplified arrangement compared with the quaternary ammonium salts: complex **5b** corresponds to **3b** but the minimum corresponding to **3c** is absent; furthermore, there is only the dimer **5c** (corresponding to **4a**) while the minima corresponding to **4b**, **4c**, **4d** and **4e** are absent.

Author contributions

Data Curation: I.A. Writing- original draft: J.E. Writing - review & editing: G.S.D, H.H.L., I. A, J.E.

Declaration of Competing Interest

The authors declare that they have no known competing financial interests or personal relationships that could have appeared to influence the work reported in this paper.

Acknowledgments

This work was carried out with financial support from the Ministerio de Ciencia, Innovación y Universidades of Spain (Project No. PGC2018-094644-B-C22) and Comunidad Autónoma de Madrid (P2018/EMT-4329 AIRTEC-CM). Thanks are also given to the CTI (CSIC) for their continued computational support.

Appendix A. Supplementary material

Supplementary data to this article can be found online at <https://doi.org/10.1016/j.cplett.2021.138809>.

References

- [1] A. Späth, B. König, Beilstein J. Org. Chem. 6 (2010) 32.
- [2] F. Bures, Top. Curr. Chem. 377 (2019) 14.
- [3] N.K. Beyeh, F. Pan, A. Valkonen, K. Rissanen, CrystEngComm 17 (2015) 1182.
- [4] E.K. Ralph, W.R. Gilkerson, J. Am. Chem. Soc. 86 (1964) 4783.
- [5] H.W. Aitken, W.R. Gilkerson, J. Am. Chem. Soc. 95 (1973) 8551.
- [6] G.S. Denisov, E.V. Ryl'tsev, D.N. Suglobov, Proc. Acad. Sci. USSR 164 (1965) 736.
- [7] G.S. Denisov, Kh.P. Oya, E.V. Ryl'tsev, D.N. Suglobov, Theor. Exp. Chem. 5 (1969) 254.
- [8] S.F. Bureiko, N.S. Golubev, G.S. Denisov, Sov. J. Chem. Phys. 3 (1985) 373.
- [9] W.E. Keder, L.L. Burger, J. Chem. Phys. 69 (1965) 3075.
- [10] C.G. Hoelger, H.H. Limbach, J. Phys. Chem. 98 (1994) 11803.
- [11] Q.R. Huang, R. Shishido, C.K. Lin, C.W. Tsai, J.A. Tan, A. Fujii, J.L. Kuo, Angew. Chem. Int. Ed. 60 (2021) 19336.
- [12] G.S. Denisov, E.V. Ryl'tsev, D.N. Suglobov, Opt. Spectrosc. 23 (1968) 338.
- [13] K.O. Christe, W.W. Wilson, R.D. Wilson, R. Bau, J.A. Feng, J. Am. Chem. Soc. 112 (1990) 7619.
- [14] C.W.F.T. Pistorius, A.A.V. Gibson, J. Solid State Chem. 8 (1973) 126.
- [15] B. Lygo, B.I. Andrews, Acc. Chem. Res. 37 (2004) 518.
- [16] J.M. Lehn, R. Meric, J.P. Vigneron, M. Cesario, J. Guilhem, C. Pascard, Z. Asfari, J. Vicens, Supramol. Chem. 5 (1995) 97.
- [17] A.S. Davies, W.O. George, S.T. Howard, Phys. Chem. Chem. Phys. 5 (2003) 4533.
- [18] D. Dong, J.B. Hooper, D. Bedrov, J. Phys. Chem. B 121 (2017) 4853.
- [19] E.V. Dalessandro, J.R. Pliego, Theor. Chem. Acc. 139 (2020) 27.
- [20] X. Xu, Q. Zhang, R.P. Müller, W.A. Goddard, J. Chem. Phys. 122 (2005), 014105.
- [21] M.P. Anderson, P. Uvdal, J. Phys. Chem. A 109 (2005) 2937.
- [22] Gaussian 16, Revision A.03, M. J. Frisch, G. W. Trucks, H. B. Schlegel, G. E. Scuseria, M. A. Robb, J. R. Cheeseman, G. Scalmani, V. Barone, G. A. Petersson, H. Nakatsuji, X. Li, M. Caricato, A. V. Marenich, J. Bloino, B. G. Janesko, R. Gomperts, B. Mennucci, H. P. Hratchian, J. V. Ortiz, A. F. Izmaylov, J. L. Sonnenberg, D. Williams-Young, F. Ding, F. Lipparini, F. Egidi, J. Goings, B. Peng, A. Petrone, T. Henderson, D. Ranasinghe, V. G. Zakrzewski, J. Gao, N. Rega, G. Zheng, W. Liang, M. Hada, M. Ehara, K. Toyota, R. Fukuda, J. Hasegawa, M. Ishida, T. Nakajima, Y. Honda, O. Kitao, H. Nakai, T. Vreven, K. Throssell, J. A. Montgomery, Jr., J. E. Peralta, F. Ogliaro, M. J. Bearpark, J. J. Heyd, E. N. Brothers, K. N. Kudin, V. N. Staroverov, T. A. Keith, R. Kobayashi, J. Normand, K. Raghavachari, A. P. Rendell, J. C. Burant, S. S. Iyengar, J. Tomasi, M. Cossi, J. M. Millam, M. Klene, C. Adamo,

- R. Cammi, J. W. Ochterski, R. L. Martin, K. Morokuma, O. Farkas, J. B. Foresman, and D. J. Fox, Gaussian, Inc., Wallingford CT, 2016.
- [23] R.F.W. Bader, *Atoms in Molecules: A Quantum Theory*, Clarendon Press, Oxford, 1990.
- [24] P.L.A. Popelier, *Atoms In Molecules, An introduction*, Prentice Hall, Harlow, England, 2000.
- [25] M.A. Blanco, A. Martín Pendás, E. Francisco, *J. Chem. Theor. Comput.* 1 (2005) 1096.
- [26] T.A. Keith, AIMAll. TK Gristmill Software, Overland Park KS, USA, Version 19.10.12, (aim.tkgristmill.com).
- [27] A.K. Pathak, T. Mukherjee, D.K. Maity, *J. Phys. Chem. A* 114 (2010) 721.
- [28] J. Autschbach, *J. Chem. Phys.* 136 (2012), 150902.
- [29] A. Kornath, F. Neumann, H. Oberhammer, *Inorg. Chem.* 42 (2003) 2894.
- [30] A.C. Legon, C.A. Rego, *J. Chem. Phys.* 99 (1993) 1463.
- [31] J. Bevirt, K. Chapman, D. Crittenden, M.J.T. Jordan, J.E. Del Bene, *J. Phys. Chem. A* 105 (2001) 3371.
- [32] B. Lakshmi, A.G. Samuelson, K.V.J. Jose, S.R. Gadre, E. Arunan, *New J. Chem.* 29 (2005) 371.
- [33] J. Luo, O. Conrad, I.F.J. Vankelecom, *J. Mat. Chem.* 22 (2012) 20574.
- [34] P. Dem'yanov, P. Polestshuk, *Chem. Eur. J.* 18 (2012) 4982.
- [35] A.M. Pendás, J.L. Casals-Sainz, E. Francisco, *Chem. Eur. J.* 25 (2019) 309.
- [36] I. Mata, I. Alkorta, E. Molins, E. Espinosa, *ChemPhysChem* 13 (2012) 1421.
- [37] D. Quiñero, I. Alkorta, J. Elguero, *Phys. Chem. Chem. Phys.* 18 (2016) 27939.
- [38] I. Alkorta, I. Mata, E. Molins, E. Espinosa, *Chem. Eur. J.* 22 (2016) 9226.
- [39] F.H. Allen, *Acta Crystallogr. Sect. B* 58 (2002) 380. F.H. Allen, W.D.S. Motherwell, *Acta Crystallogr. Sect. B* 58 (2002) 407.
- [40] M. Bolte, CSD Communication (2020).
- [41] Z. Gao, Y. Wu, Z. Tang, X. Sun, Z. Yang, H.L. Cai, X.S. Wu, *J. Mater. Chem. C* 8 (2020) 5868.
- [42] U. Böhme, M. Gerwig, CSD Private communication (2018).
- [43] J.K. Cockcroft, A. Shamsabadi, H. Wu, A.R. Rennie, *Phys. Chem. Chem. Phys.* 21 (2019) 25945.
- [44] I. Alkorta, J. Elguero, A. Frontera, *Crystals* 10 (2020) 180.